



Budapest University of Technology and Economics
Faculty of Electrical Engineering and Informatics

MODELING AND CHARACTERIZATION OF INTEGRATED MICROSCALE HEATSINK STRUCTURES

Ph. D. thesis booklet

Author: TAKÁCS Gábor

Advisor: Dr. BOGNÁR György, Ph.D.

Department of Electron Devices
Budapest, 2017.

1 Introduction

The limiting factor of the integration of electronic devices is the overheating of the devices themselves that is caused by the increasing dissipation density [1]. Thanks to the advances in CMOS technology (FinFET, Tri-Gate, SOi, low-K, etc.) to decrease the dissipation, it is possible to meet the demands of Moore's Law to increase the number of integrated components (gates, transistors) per unit area without the significant increase of dissipation. However, as a consequence of the More-than-Moore integration (3D packaging, System-in-Package, System-on-Package, etc.) the dissipation per unit area can exceed the single chip dissipation multiple times.[1].

As a consequence of the 3D integration the chip-to-ambient heat flow path has become significantly "longer", thus the temperature of the ICs' increased drastically. This can be explained by the increased junction-to-package and junction-to-ambient thermal resistances that lead to increased temperature on the surface of the chips, even when the exact same surface dissipation was applied. Since it is of great importance to cope with the effects of increased temperature even in the early design phases, it is vital to develop compact thermal models that incorporates the effects and characteristics of SoP devices and integrated microscale heatsink structures.

All these reasons indicates, that in case of 3D integration, special attention must be paid for thermal management issues, responsible for increasing the performance, reliability and robustness of modern devices further.

In case of System-on-Package devices, the role of the interposer is not only to realize the connection between the integrated circuit and the printed circuit board but additional passive devices (resistances, capacitors, embedded inductances) can be created inside it. There is a lot of ongoing research where devices with additional functionalities are integrated in the interposer: accumulators, sensors and actuators, cooling systems, etc. In certain cases, the integration of cooling solutions with microchannels are investigated.

By circulating cooling fluid in these microchannels the junction-to-package thermal resistance can be dramatically decreased – that depends on the substance of the fluid and the flow type.

The best way to decrease the length of the heat flow path and thus the overall thermal resistance is to create microchannels on the backside of the chips [2]. The channels can be created with varying layout and geometry and by using different manufacturing technologies like reactive ion etching, wet etching, etc. However, to create a device to transfer as much heat as possible – to maximize the cooling efficiency - within the size limitations, the proper understanding of the heat transfer mechanisms is necessary.

2 Research aims and objectives

The inner motivation to find the solution for the thermal problems and other issues concerning the microchannel heatsinks was the driving force that lead and accompanied me during my doctoral research. My supervisor Dr. György Bognár dealt with the thermal transient characterization of microchannel heatsinks in the 3rd thesis in his dissertation that was successfully defended in 2009 [3]. He stated that the thermal transient method is applicable to determine the R_{thjc} junction-to case thermal resistance. As a result, a flow rate dependent, 2nd order approximation model was created based on his measurements at different flow rates.

One of the aims of my research is to develop an analytical model that calculates the heat transfer in the microchannels by knowing the relevant heat transfer parameters – flow rate, material properties. Despite the fact that the heat transfer is an important parameter – that is described by the heat transfer coefficient – it is not commonly used in everyday engineering practice. Mostly, the thermal resistance of the device determines the dissipation corresponding to the maximal temperature. It is important to validate the analytical model within its range of validity. One way of the validation is to check the results by numerical simulations. In order to do so, I have conducted finite volume method based computational fluid dynamics simulations by using the 3D model of the device. Beside the model validation, the simulations have another purpose: they helped the qualitative understanding of the heat transport mechanism in the microchannels with the several visualizations capabilities (temperature distribution map, flux-density map). In addition, they also helped during the model simplification phase.

In the next part of my work, I am dealing with measurement issues. My goal is to create a measurement system that is suitable to thermally characterize microchannel heatsink devices, which means it can determine the fluid flow rate dependent thermal resistance of the device. However, contrary to the work of my supervisor, I am planning to create a measurement method which is suitable to determine the heat transfer through the walls of the microchannels that differs less than 10% from the results of the analytical expression validated by simulations.

3 Applied tools and inspection methodologies

– **Gas flow control:** During the measurement I applied an Alicat MC-10SLPM-D/10V, 10IN, GAS:Air gas flow controller. This instrument was calibrated by the vendor. It has the accuracy of 0.8% of reading and 0.2% of full scale. The turndown ratio is 200:1, the maximum flow rate is 600 liter/h (10 liter/min). Warm-up time is less than 1 second. The calibration certificate is available.

– **Refrigerated and heating circulators:** To provide the stable temperature of the cold plate I applied a Julabo F25 Refrigerated and heating circulator device. The temperature stability is 0.01 °C. The cooling capacity at 20 °C is 350W.

– **Digital temperature meter:** To measure the temperature I used an Omega HH806AU digital hand-held temperature meter. The measurement range is -200 °C-1372 °C. The uncertainty is $\pm 0.05\% + 0.3$ °C reading error.

– **Optical microscope:** To measure the physical geometry of the microchannel-based heat sink I used an Olympus BX51 optical microscope.

– **Computer aided three dimensional design software:** The 3D models were designed using Catia V5R20 (Computer Aided Three Dimensional Interactive Application). In the software I used micro scale which is developed for MEMS (Micro Electro Mechanical System) design.

– **Thermal transient tester:** For the thermal transient testing I used a T3Ster thermal transient tester device [4] and its software tool. The accuracy based on the resolution of time and the resolution of the voltage measurement. The maximal sampling rate is 1 MSPS, the resolution is 12 bits, thus the voltage step is 12 μ V. At K-factor of -2mV/K the temperature resolution is 0.01 °C. For the evaluation of the measurement results I applied the T3Ster Master v2.1 software.

– **Matemathical softwares:** I used Maple 9 and MATLAB 2015b. Later it was updated to MATLAB 2017b-re.

– **Simulation softwares:** I used two softwares for numerical simulations: Mentor Graphics) FloTHERM [5], and ANSYS CFX simulator tool [6].

3.1 The experimental sample of microchannel heat sink

To validate the results of the analytical model I used a previously manufactured prototype sample of the microchannel heat sink.

The integrated microchannel heat sink was processed by wet anisotropic etching of <100> n-type silicon wafers in tetramethyl-ammonium-hydroxide (TMAH). The etching was performed in a 25 % solution of TMAH at 85°C resulting in an etch speed of ca. 0.3 microns/minute. The etching solution contained no additives and was performed in an ultrasonic bath. Due to the ultrasonic bath the bubbles formed during etching are quickly removed from the silicon surface. This ensures homogeneous etching even in case of batch processing. In addition, the combination of ultrasonic excitation and slow etch speed results in a very low surface roughness.

The experimental samples were formed in 2" single side polished wafers, 4 structures with the size of 15 × 15 mm on each wafer. The channels were etched on the polished surface in radial directions. At the intersection – in the middle of the chip – a cavity of ca. 4 mm in diameter was formed for the gas inlet. The main idea behind the channel topology is based on a previous research which was done together with Heriot-Watt University, Edinburgh, Scotland [7]–[9] project of FP6 PATENT DfMM EU 507255. These studies can also be utilized to compare the performance

of the two structures against one another. Finally, the wafers were diced and the channels on the polished side of the wafer were closed with borofloat 33 glass attached by anodic wafer bonding. For the gas inlets a hole with a diameter of 2 mm was cut into the closing glass substrate with laser.

Due to the anisotropic etching process the channel geometries were different in different directions. Thanks to the rotation symmetry there are only 12 different channels.

4 New scientific results

4.1 Compact model of the microchannel-based heat sink

My goal was to develop a formula which can be utilized at laminar, transition and turbulent types of flow with different Nusselt-function. The analytical formula describes the heat transfer in a single straight microchannel. The partial thermal resistance which describes the heat transfer in a microchannel can be calculated as

$$R_{Th} = \frac{1}{\frac{dm}{dt} \cdot c_p \cdot \left(1 - e^{-\frac{h \cdot A}{\frac{dm}{dt} \cdot c_p}}\right)}$$

where $\frac{dm}{dt}$ is the mass flow, c_p is the specific heat and A is the area. In this equation, the h parameter is the heat transfer coefficient which depends on the fluid properties. It can be calculated as

$$h = \frac{k_f \cdot Nu}{D_H}$$

The Nusselt- number can be determined by applying

$$Nu = Nu_{\infty} + \frac{0.065 \cdot (D_H/L) \cdot Re \cdot Pr}{1 + 0.04 \cdot [(D_H/L) \cdot Re \cdot Pr]^{\frac{2}{3}}}$$

for laminar flow and constant wall temperature [10], where Nu_{∞} is the Nusselt-number for infinite long channel, Re is the Reynolds-number, Pr is the Prandtl-number, D_H is the hydrodynamic diameter and L is the channel length. Nu_{∞} can be calculated as

$$Nu_{\infty} = -0.0274 \cdot \left(\frac{a}{b}\right)^2 + 0.631 \cdot \left(\frac{a}{b}\right) + 2.3224$$

where $\frac{a}{b}$ is the aspect ratio of the cross section of the channel.

4.1.1 Region of validity of the compact model

It was essential to define the region of the validity of the novel thermal compact model. The proposed model is independent from the type of flow, but the suggested Nusselt function can only be applied in case of laminar flow. For another type of flow one can apply different Nusselt-function in this model.

Increasing fluid flow velocity to achieve the turbulent region requires high pressure drop which requires high pumping power. At high fluid flow velocity the physical properties of the fluid cannot be assumed as constant along the channel which phenomenon has to be taken into consideration.

The proposed analytical model is valid below the fluid flow speed of 1/3 Mach. Above this velocity, the model can give false results despite the proper Nusselt-function.

The microchannels have to be longer than the hydrodynamic channel length.

The region of validity is also limited by the Knudsen-number which has to be less than 0.1. This is essential due to the validity of the continuity equations. For air flow at room temperature it means the free path of the air molecules is 0.07 μm , so the minimal hydrodynamic diameter is 0.7 μm .

4.1.2 Numerical investigation of heat transfer

I utilized the analytical compact thermal model to determine the flow-rate dependent partial thermal resistance at different flow rate, the results can be find in Table 1. To validate these results I also performed CFD (Computational Fluid Dynamics) simulations.

Table 1. Comparison of the calculated and simulated thermal resistances at different flow rate

Flow rate [l/h]	Calculated thermal resistance [K/W]	Simulated thermal resistance [K/W]	Deviation
30	99.1	103	3.8%
60	49.6	51.1	3.5%
90	33.4	34.4	2.9%
120	25.6	26	1.5%

I compared the results of the analytical model and the partial thermal resistances of the finite volume simulations, which are in a good agreement as it can be seen in Table 1. The highest deviation is at the flow rate of 30 liter/hour, which is only 3.8%.

My results are summarized in Thesis I.

Thesis I. I have developed a closed analytical formula to determine the partial thermal resistance of microchannel-based heat sinks, which takes into consideration the channel geometry together with the physical and the flow properties of the working fluid. The model is valid if the channel wall temperature is constant, the flow type is laminar, the fluid flow velocity is lower than 1/3 Mach, and the channel length is longer than the hydrodynamic entry length. I have applied the formula on a complex, microchannel-based heat sink to calculate the partial thermal resistance. The results are validated by finite volume simulations. [J4, J6, C1, C3, C4, C7]

4.2 Development of a novel measurement methodology for heat transfer

The description of the measurement methodology can be found in JEDEC JEST 51 standard [11]. The JESD 51-1 contains the measurement guideline for a single semiconductor device. The JESD 51-2 summarizes the requirements for ambient conditions. The measurement methodology for forced convection cooled devices can be found in JESD-51-6 standard. This standard does not cover the measurement of cooling efficiency for integrated microchannel cooling. Recently there is not any standardized thermal transient testing based measurement methodology.

The thermal model of the developed measurement setup can be seen in Figure 1 where ($R_{th,induced}$) is the parallel heat flow path caused by the air circulation around the measurement setup induced by the outflowing working fluid.

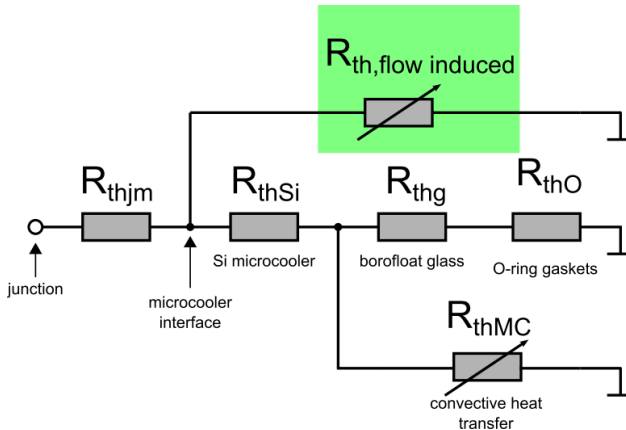


Figure 1. Thermal model of the measurement

I performed finite volume simulations to analyze the effect of the outer air movement, which caused high uncertainty in the measurements.

Applying the formula based on the thermal model of the measurement setup the partial thermal resistance can be determined. These results are compared with the results of the analytical model and the results of the finite volume simulations. The deviations are also calculated. The results can be found in Table 2.

Table 2 Comparison of the calculated, simulated and measured results

Flow rate [l/h]	Calculated thermal resistance [K/W]	Simulated thermal resistance [K/W]	Measured thermal resistance [K/W]	Deviation
30	99.1	103	92.2	8%
60	49.6	51.1	49.9	1%
90	33.4	34.4	34.9	2.8%
120	25.6	26	26.9	4.3%

The deviation of the measurement results are less than 10% compared to the finite volume method and any the result of the analytical model.

Thesis II. *I have developed a novel, thermal transient testing based measurement method to measure the heat transfer in microchannels of microchannel-based heat sinks. I have identified some measurement uncertainties in case of discrete microchannel-based heat sinks. I have proved that most of the measurement uncertainties are caused by the heat transfer in the intake manifold and by the induced outer air circulation. I have suggested a novel measurement setup, which is designed to reduce the aforementioned phenomena. I have measured the partial thermal resistance of a microchannel-based heat sink with complex channel geometry. The measurement results are compared with the results of the analytical calculations and finite volume simulations. [J1, J3, J5, J7, C2, C5]*

4.3 Determining the proper channel length

The proposed method can be used if the channel length is longer than the thermal entry length. The maximum removable energy per unit time, i.e. maximum heat flow is determined by the conservation of energy equation for the steady flow of coolant in channels:

$$\frac{dQ_{max}}{dt} = \frac{dm}{dt} \cdot c_p \cdot (T_w - T_i) \left(1 - e^{-\frac{L}{L_{char}}} \right),$$

where $(T_w - T_i)$ is the temperature difference between the wall of channel and the temperature of the fluid when it enters. Because the average Nusselt number (thus the average heat transfer coefficient also) depends on the L length of the channel, the L_{char} characteristic channel length is

$$L_{char} = \frac{\frac{dm}{dt} C_p}{h \cdot p}$$

This value exactly represents the distance between the channel entrance and the point where the mean fluid temperature reaches 63% of the wall temperature.

I utilized the proposed method on the experimental sample and I determined the characteristic channel length. The results can be find in Table 3.

Table 3 Calculated characteristic channel lengths

Cumulative flow rate [l/h]	Flow rate per channel [l/h]	Calculated characteristic channel length [mm]
30	0.625	0.189
60	1.500	0.371
90	1.875	0.560
120	2.500	0.747
240	5.000	1.494

It can be seen that at low flow rated the characteristic channel length is quite short, even at 120 liter/hour is shorter than one millimeter.

To validate the analytical model I performed finite volume simulations. I developed an algorithm to get the heat flux density map, which can be seen in Figure 2. Under the inlet, there is a stagnation point where the heat transfer is close to zero. The heat density map also proves that the most of the heat transferred close to the inlet, which is in good agreement with the prediction of the analytical model.

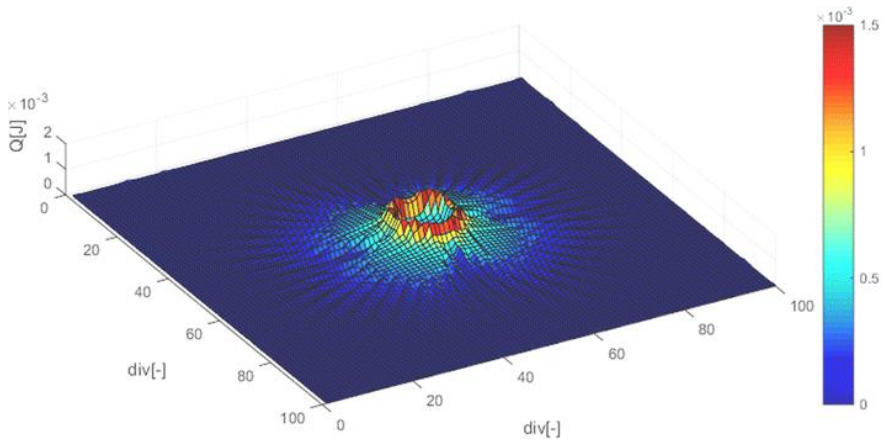


Figure 2 Heat flux density map

To validate the proposed method I performed further simulation. I analyzed only a single channel to speed up the work. The given results can be seen in Table 4, where they are compared with the calculated ones. The deviations are also calculated.

Table 4 Comparison of calculated and simulated characteristic lengths

Cumulative flow rate [l/h]	Calculated characteristic length [mm]	Simulated characteristic length [mm]	Deviation [mm]	Deviation [%]
30	0.189	0.18	0.009	5
60	0.371	0.35	0.021	6
90	0.560	0.56	0	0
120	0.747	0.75	-0.003	-0.4
240	1.494	1.50	-0.006	-0.4

The deviation remained less than 10% in the whole range. The proposed method can be extended to the transition and turbulent flow region, but in this case, the proposed Nusselt-function is not valid anymore.

Thesis III. *I have developed a methodology to determine the proper channel length of a microchannel-based heatsinks, which takes into consideration the fluid flow properties and the channel geometry. I have introduced the concept of the characteristic channel length (L_{char}) which defines the channel length where fraction of $1-1/e$ of the transferrable heat quantity is transferred. I have applied this methodology on a microchannel-based heatsink with complex geometry and I have proved that only the 31.3 percent of the area is necessary to utilize the 95 percent of the maximal transferrable amount of heat ($3 \times L_{char}$). I have validated the methodology using finite volume simulations. [J2, C6]*

5 Applications of the results

The research was conducted within the framework of the K 109232 project of the Hungarian Scientific Research Fund (OTKA) entitled “Integrated thermal management in System-on-Package devices”. Based on the results of the first 4 years the auditing committee classified the work of our research team as “successful”.

The model, I have elaborated, was validated by measurements and FVM simulations, which allows it use in coupled thermo-hydrodynamics simulators. An enhanced version of my model was integrated into a novel thermal simulator and the results and the applicability of the simulator was published in a conference paper in a prestigious international conference [C7].

I have proved that the elaborated measurement technique is suitable to meter the heat transfer in microchannels. Thanks to this, I have acquired an equipment that is suitable to measure and distinguish the heat transport even in the critical and the transition ranges. For this kind of measurement, experimental devices with simplified geometries are necessary. In order to meet these requirements, the design and manufacturing of the devices are done and the applicability of the analytical model was extended for turbulent flows types. The corresponding results were published in an international journal paper [J6].

The elaborated method of microchannel heatsink development is not only suitable for integrated circuit cooling, but it is also applicable on a broader scale. An example was published in [C6], where concentrated photovoltaics solar cell was cooled using microchannel-based heatsink structures. The design of the channel geometry and the value of the required fluid flow rate was determined by using my method (determination of the optimal channel length).

According to my suggestions, the measurement setup was redesigned to be suitable for liquid cooling as well with the same benefits that described the gas cooling. However, the construction is still ongoing during my thesis writing.

Publications – Journal papers

- [J1] G. Takács, P. G. Szabó, B. Plesz, Gy. Bognár. Improved thermal characterization method of integrated microscale heat sinks. **MICROELECTRONICS JOURNAL** **45**:(12) pp. 1740-1745. (2014)
- [J2] G. Takács, P. G. Szabó, Gy. Bognár. Thermal management in System-on-Package structures by applying microscale heat sink. Part I: Consideration of the appropriate channel length of microscale heat sink(s). **MICROELECTRONICS JOURNAL** **46**:(12 A) pp. 1202-1207. (2015)
- [J3] G. Takács, P. G. Szabó, Gy. Bognár. Enhanced thermal characterization method of microscale heatsink structures. **MICROELECTRONICS RELIABILITY** **67**:(-) pp. 21-28. (2016)
- [J4] G. Takács, P. G. Szabó, Gy. Bognár. Modeling of the flow-rate dependent partial thermal resistance of integrated microscale cooling structures. **MICROSYSTEM TECHNOLOGIES** **23**:(9) pp. 4001-4010. (2017)
- [J5] Márton Németh , Gábor Takács, Lázár Jani , András Poppe. Compact modeling approach for microchannel cooling and its validation. **MICROSYSTEM TECHNOLOGIES** **23**: Paper MITE-D-16-00550R.13 p. (2017)
- [J6] Gy. Bognár, G. Takács, L. Pohl, P. G. Szabó. Thermal modeling of integrated microscale heatsink structures. **MICROSYSTEM TECHNOLOGIES** -:(-) pp. 1-12. (2017)
- [J7] Gábor Takács, György Bognár, Enikő Bándy, Gábor Rózsás, Péter G. Szabó. Fabrication and Characterization of Microscale Heat Sinks. **MICROELECTRONICS RELIABILITY** -:(-) pp. 1-8. (2017)

Publications – Conference papers

- [C1] Takács Gábor, Bognár György, Szabó Péter Gábor. Hőátadási jelenségek vizsgálata mikroméretű csatornákat tartalmazó integrált hűtőeszközökben. In: Keresztes Gábor (szerk.). Tavasz Szél 2015 / Spring Wind 2015 Konferenciakötet: III. kötet. Konferencia helye, ideje: Eger, Magyarország, 2015.04.10-2015.04.12. Eger: Líceum Kiadó, 2015. pp. 435-446.
- [C2] G. Takács, P. G. Szabó, Gy. Bognár. Enhanced Thermal Characterization Method of Microscale Heatsink Structures In: Chris Bailey, Bernhard Wunderle, Sebastian Volz (szerk.). Proceedings of the 21st International Workshop on THERMAL INvestigation of ICs and Systems (THERMINIC'15). Konferencia helye, ideje: Paris, Franciaország, 2015.09.30-2015.10.02. Paris: pp. 1-4.
- [C3] G. Takács, P. G. Szabó, Gy. Bognár. Modeling of the flow rate dependent partial thermal resistance of integrated microscale cooling structures. In: Charlot B, Mita Y, Nouet P, Presseccq F, Schropfer G, Rencz M, Schneider P

- (szerk.). Proceedings of the Symposium on Design, Test, Integration and Packaging of MEMS/MOEMS (DTIP'15). Konferencia helye, ideje: Montpellier, Franciaország, 2015.04.27-2015.04.30. New York: IEEE, 2015. pp. 252-255.
- [C4] Gy. Bognár, G. Takács, L. Pohl, P. G. Szabó. Thermal modeling of integrated heatsink structures. In: B Charlot, Y Mita, P Nouet, F Pressecq, M Rencz, P Schneider, N Tas (szerk.). Proceedings of the Symposium on Design, Test, Integration and Packaging of MEMS/MOEMS (DTIP'16). 347 p. Konferencia helye, ideje: Budapest, Magyarország, 2016.05.30-2016.06.02. New York: IEEE, 2016. pp. 173-177.
- [C5] Gábor Takács, György Bognár, Enikő Bándy, Gábor Rózsás, Péter G. Szabó. Fabrication and Characterization of Microscale Heat Sinks. In: András Poppe (szerk.). Proceedings of the 22nd International Workshop on THERMal INvestigation of ICs and Systems (THERMINIC'16). 349 p. Konferencia helye, ideje: Budapest, Magyarország, 2016.09.21-2016.09.23. Budapest: BME Elektronikus Eszközök Tanszék, 2016. pp. 264-267.
- [C6] Plesz Balázs, Takács Gábor, Szabó G. Péter, Kohári Zsolt, Németh Márton, Bognár György. Integrated microscale cooling for concentrator solar cells. In: Pascal Nouet. Pascal Nouet (szerk.). Proceedings of the Symposium on Design, Test, Integration and Packaging of MEMS/MOEMS (DTIP'17). 282 p. Konferencia helye, ideje: Bordeaux, Franciaország, 2017.05.29-2017.06.01. Montpellier: University of Montpellier, 2017. pp. 158-161.
- [C7] György Bognár, Gábor Takács, László Pohl, Lázár Jani, András Timár, Péter Horváth, Márton Németh, András Poppe, Péter Gábor Szabó. Integrating Chip-level Microfluidics Cooling into System Level Design of Digital Circuits. In: Veerendra Mulay, Jesse Galloway, Adriana Rangel (szerk.). Proceedings of the 33rd IEEE Semiconductor Thermal Measurement and Management Symposium (SEMI-THERM'17). 302 p. Konferencia helye, ideje: San Jose, Amerikai Egyesült Államok, 2017.03.13-2017.03.17. San Jose: IEEE, 2017. pp. 77-87.

Publications – Not relevant in terms of theses

- [N1] Gy. Bognár, P.G. Szabó, G. Takács. Generalization of the thermal model of infrared radiation sensors. MICROELECTRONICS JOURNAL 46:(6) pp. 543-550. (2015)
- [N2] T Garami, G Takacs, O Krammer, A Szabo. Investigation of the pre-heating process during thermosonic wire bonding by FEM simulation. In: J Nicholics (szerk.). 38th International Spring Seminar on Electronics Technology (ISSE). Konferencia helye, ideje: Eger, Magyarország, 2015.05.06-2015.05.10. (IEEE). New York: IEEE, 2015. pp. 333-338

References

- [1] L. Sauciuc, G. Chrysler, R. Mahajan, and M. Szeleper, "Air-cooling extension-performance limits for processor cooling applications," in *Semiconductor Thermal Measurement and Management Symposium, 2003. Nineteenth Annual IEEE*, 2003, pp. 74–81.
- [2] D. B. Tuckerman and R. F. W. Pease, "High-performance heat sinking for VLSI," *IEEE Electron Device Lett.*, vol. 2, no. 5, pp. 126–129, 1981.
- [3] Dr. Bognár György, "A mikroelektronika egyes termikus problémáinak kezelése," Budapesti Műszaki és Gazdaságtudományi Egyetem, 2009.
- [4] "T3Ster - Thermal characterization of IC packages, LEDs and systems - Mentor Graphics." [Online]. Available: <https://www.mentor.com/products/mechanical/micred/t3ster/>. [Accessed: 06-Nov-2017].
- [5] "FloTHERM - Electronics thermal analysis software - Mentor Graphics." [Online]. Available: <https://www.mentor.com/products/mechanical/flotherm/flotherm/>. [Accessed: 08-Nov-2017].
- [6] "ANSYS CFX: Turbomachinery CFD Simulation." [Online]. Available: <http://www.ansys.com/Products/Fluids/ANSYS-CFX>. [Accessed: 08-Nov-2017].
- [7] Z. Kohári, G. Bognár, G. Horváth, A. Poppe, M. Rencz, and V. Székely, "Cross-verification of thermal characterization of a microcooler," *J. Electron. Packag.*, vol. 129, no. 2, pp. 167–171, 2007.
- [8] M. P. Y. Desmulliez, A. J. Pang, M. Leonard, R. S. Dhariwal, W. Yu, E. Abraham, G. Bognár, A. Poppe, G. Horvath, Z. Kohari, M. Rencz, D. Emerson, R. W. Barber, O. Slattery, F. Waldron, and N. Cordero, "Fabrication and characterization of a low-cost, wafer-scale radial microchannel cooling plate," *IEEE Trans. Components Packag. Technol.*, vol. 32, no. 1, pp. 20–29, 2009.
- [9] W. Yu, M. P. Y. Desmulliez, A. Drufke, M. Leonard, R. S. Dhariwal, D. Flynn, G. Bognár, A. Poppe, G. Horvath, Z. Kohari, and M. Rencz, "High-aspect-ratio metal microchannel plates for microelectronic cooling applications," *J. Micromechanics Microengineering*, vol. 20, no. 2, p. 25004, 2010.
- [10] A. F. Edwards, D. K., Denny, V. E., Mills, *Transfer Processes*. Hemisphere, 1979.
- [11] "METHODOLOGY FOR THE THERMAL MEASUREMENT OF COMPONENT PACKAGES (SINGLE SEMICONDUCTOR DEVICE) | JEDEC." [Online]. Available: <https://www.jedec.org/standards-documents/docs/jesd-51>. [Accessed: 05-Nov-2017].